Electrocatalytic oxidation of formic acid by Pt/Co nanoparticles

Ning Chi, Kwong-Yu Chan and David Lee Phillips

Department of Chemistry, The University of Hong Kong, Pokfulam Road, Hong Kong, SAR of China
E-mail: chemmail@hku.hk

Received 4 June 2000; accepted 31 October 2000

The electrocatalytic activity of Pt/Co bimetallic nanoparticles towards formic acid (0.2 M HCOONa/0.28 M $HClO_4$) oxidation was explored by cyclic voltammetry of the nanoparticles supported on highly oriented pyrolytic graphite (HOPG). The particles were prepared by electrodeposition from a bath of mixed concentrations of Co^{2+} and $PtCl_6^{2-}$ ions and characterized by tapping mode atomic force microscopy (TMAFM). The compositions of the nanoparticles were determined as close as possible to individual particles by energy dispersive X-ray analysis (EDX). Nanoparticles of different atomic ratios of Pt/Co were prepared and the peak currents in cyclic voltammetry of formic acid oxidation were measured. The activity of the bimetallic particles was found to be maximum when the atom ratio Pt : Co is between 1 : 1.1 and 1 : 3.5. The maximum activity is about one order of magnitude higher than that of pure Pt nanoparticles. Comparison of the currents to those from microelectrodes and wire electrodes shows no mass-transfer limitations in nanoparticles with diameters less than 100 nm. The bimetallic particles exhibit interesting kinetics and Co appears to significantly enhance the electroxidation of formic acid. The advantage of using nanoparticles for mass-transfer free kinetics studies is also demonstrated.

KEY WORDS: electrocatalysis; nanoparticles; bimetallic particles; Pt/Co; Pt particles

1. Introduction

Platinum is a versatile but expensive catalyst. There has been a great deal of interest in studies of platinum catalysis at the nanoparticle level in order to optimize the use of Pt as a catalyst. This is particularly important in electrocatalysis and commercialization of fuel cells since platinum is vital for both anodic oxidation of small organic molecules and cathodic reduction of oxygen. Previous studies of electrocatalysis of platinum nanoparticles [1,2] displayed inconsistent results since the porous electrode support was not well characterized and there could be inherent mass-transfer effects. Platinum nanoparticles prepared on single-crystal metal surfaces are prone to reconstruction with the surface whereas other well-defined surfaces such as mica are nonconducting. Preparation and characterization of platinum nanoparticles on HOPG have recently been reported [3–5] and this provides the opportunity for detailed electrocatalysis studies. The activity of platinum towards electrooxidation of small organic molecules can be promoted by introduction of a second or third metal [6–11]. It is desirable to perform kinetics studies of mixed metals with their composition characterized at the nanoparticle level. Determination of an optimal atomic ratio for mixed metal catalysts will lead to further optimization of platinum usage in catalysts.

In this paper, the kinetics of pure platinum nanoparticles and mixed platinum/cobalt nanoparticles towards formic acid oxidation are reported. The nanoparticles are prepared by electrodeposition and characterized by tapping mode atomic force microscopy (TMAFM) in a procedure similar to those previously reported [3,4]. The cyclic voltammograms of formic acid oxidation on Pt wire, Pt microelectrodes, Pt nanoparticles, Pt/Co deposited microelectrodes, and Pt/Co nanoparticles, were carried out and the peak oxidation currents obtained. The optimum ratio of Pt : Co for maximum activity was identified. The mass-transfer effects, the use of nanoparticles as model catalysts, and the role of Co in electroxidation of formic acid are discussed.

2. Experimental

Pt nanoparticles were deposited on newly cleaved highly oriented pyrolytic graphite (HOPG) from hexachloroplatinic acid in aqueous or acetonitrile solution at room temperature. The procedure was similar to that described previously [3,4]. Bimetallic Pt/Co nanoparticles were co-deposited from aqueous solutions of 2.5 mM H_2PtCl_6 and various concentrations of $CoCl_2$. A.R. grade chemicals and Milli-Q water (18.2 MΩ cm) were used. Formic acid was prepared by acidifying 0.2 M HCOONa solution with 0.28 M $HClO_4$. The oxidation current, in the sub-microampere range, was measured in a faraday cage to minimize electromagnetic disturbance. Electrochemical deposition and voltammetry experiments were carried out with an EG&G PAR 263 potentiostat/galvanostat. A Ag/AgCl electrode with a 3.0 M KCl solution was used as the reference electrode. Pt and Pt/Co nanoparticles deposited on HOPG were imaged by a Digital Instruments Nanoscope-IIIA atomic force microscope (AFM) operating in air the tapping mode. The surface area of Pt nanoparticles was estimated from the digital images of the TMAFM by counting the number of particles and measuring their two-dimensional diameters. To calculate the surface area, the particles were assumed to be hemispheri-

cal in shape. This assumption will overestimate the surface area a bit since from the height data, the particles are somewhat two dimensional and not spherical. Energy dispersive X-ray analysis (EDX) was taken on Pt/Co nanoparticles using a Link Pentafet detector and a Link Analytical analyzer. The EDX analysis was performed close to individual particle level and there is little variation of composition among different particles on the same HOPG surface.

3. Results and discussion

Different compositions of Pt/Co nanoparticles were electrochemically deposited from mixed solutions of 2.5 mM H_2PtCl_6 and $CoCl_2$ of 0, 5, 30, 50, 70, 100, and 150 mM. The deposition was controlled at 1 μA and the deposition time was 3 s. The deposition conditions, resulting composition, and size of the nanoparticles are tabulated in table 1 whereas figure 1 shows the TMAFM images of some representative samples. The mean diameter and surface area increase with the $CoCl_2$ concentration. Another sample of Pt/Co nanoparticles shown in figure 1(e) were prepared with a higher current of 100 μA for 3 s from a mixed solution of 2.5 mM H_2PtCl_6 and 50 mM $CoCl_2$ for 3 s. Pure Pt nanoparticles shown in figure 1(f) were prepared in acetonitrile solution of 2.5 mM H_2PtCl_6 and a supporting electrolyte of 80 mM Et_4NCl at 1 μA for 3 s. The Co percentage of some of the nanoparticles was determined by EDX analysis focusing on individual particles. Measurements were made on at least five different particles on one sample. The spread of the composition distribution is shown in table 1 and Co composition is uniform from particle to particle on the same sample surface. It appears that Co is uniformly mixed with Pt in a particle, and not scattered into individual Co particles.

Besides supplying Co^{2+} for deposition, $CoCl_2$ also acts as additional supporting electrolyte. Sufficient supporting electrolyte can help the formation of 2D particles [3]. The TMAFM images of bimetallic nanoparticles (figure 1 (a)–(d)) tend to show an increase of 2D growth with the concentration of $CoCl_2$ in the deposition bath. For the same amount of coulombs passed, the mean size of Pt/Co nanoparticles increases with concentration of $CoCl_2$.

To investigate the kinetics of formic acid oxidation, cyclic voltammetry (CV) experiments were performed in an acidified sodium formate solution, 0.2 M HCOONa/0.28 M $HClO_4$. The CV for a 100 μm diameter platinum microelectrode at a scan rate of 100 mV/s is shown in figure 2. The high potential limit is 850 mV Ag/AgCl and two oxidation peaks are seen in the forward scan. The thermodynamic potential of the formic acid oxidation

$$\mathrm{CHOOH} \rightarrow \mathrm{CO_2} + 2\mathrm{H^+} + 2\mathrm{e} \tag{1}$$

is $E^0 = -0.126$ V vs. RHE. The first oxidation peak in figure 2 is about 0.2 V Ag/AgCl and the $E_{1/2}$ is about 0 V Ag/AgCl which is a bit higher than the standard potential of formic acid oxidation. The second oxidation peak is probably due to oxidation of the intermediates. A possible mechanism of formic acid oxidation on platinum has been proposed [12,13] as

$$\mathrm{HCOOH} \rightarrow \mathrm{COOH_{ad}} + \mathrm{H^+} + \mathrm{e^-} \tag{2}$$

$$\mathrm{HCOOH} + \mathrm{COOH_{ad}} \rightarrow \mathrm{CO_{ad}} + \mathrm{CO_2} + \mathrm{H_2O} + \mathrm{H^+} + \mathrm{e^-} \tag{3}$$

$$\mathrm{COOH_{ad}} \rightarrow \mathrm{CO_2} + \mathrm{H^+} + \mathrm{e^-} \tag{4}$$

$$\mathrm{CO_{ad}} + \mathrm{OH_{ad}} \rightarrow \mathrm{CO_2} + \mathrm{H^+} + \mathrm{e^-} \tag{5}$$

Step (2) is the rate-determining step for catalysis by pure platinum. Steps (3) and (4) are fast steps [14] but the generation of CO_{ad} can poison the platinum catalyst and the second oxidation peak may be related to oxidation of poison intermediates. In the reverse scan, there is only one oxidation peak and it has a higher current than the original first peak of the forward scan. As reported earlier [15], the presence of a second oxidation peak and a higher peak current in reverse

Table 1
Co percentage, mean diameter, surface area, and peak current density of different samples of Pt/Co nanoparticles and pure Pt nanoparticles shown in figure 1.

	Nanoparticles							
	Pt/Co Fig. 1(a)	Pt/Co	Pt/Co Fig. 1(b)	Pt/Co	Pt/Co Fig. 1(c)	Pt/Co Fig. 1(d)	Pt/Co Fig. 1(e)	Pt Fig. 1(f)
H_2PtCl_6 2.5 mM	5 mM $CoCl_2$	30 mM $CoCl_2$	50 mM $CoCl_2$	70 mM $CoCl_2$	100 mM $CoCl_2$	150 mM $CoCl_2$	50 mM $CoCl_2$	80 mM Et_4NCl
Deposition	1 μA, 3 s	1 μA, 3 s	1 μA, 3 s	1 μA, 3 s	1 μA, 3 s	1 μA, 3 s	100 μA, 3 s after air annealing	1 μA, 3 s
Pt : Co (atom)	1 : 0.50	1 : 1.10	1 : 3.46	1 : 3.63	1 : 4.43	1 : 7.40	1 : 3.46	1 : 0
Mean diameter (nm)	2D nuclei network	22.05	36.26	28.5	54.79	60.55	89.7	41.25
Surface area (cm^2)	0.02	0.021	0.0305	0.0290	0.057	0.0581	0.04435	0.0256
Peak current density j_p (mA/cm^2)	7.05	56	61	33	30	17.5	55	6.1

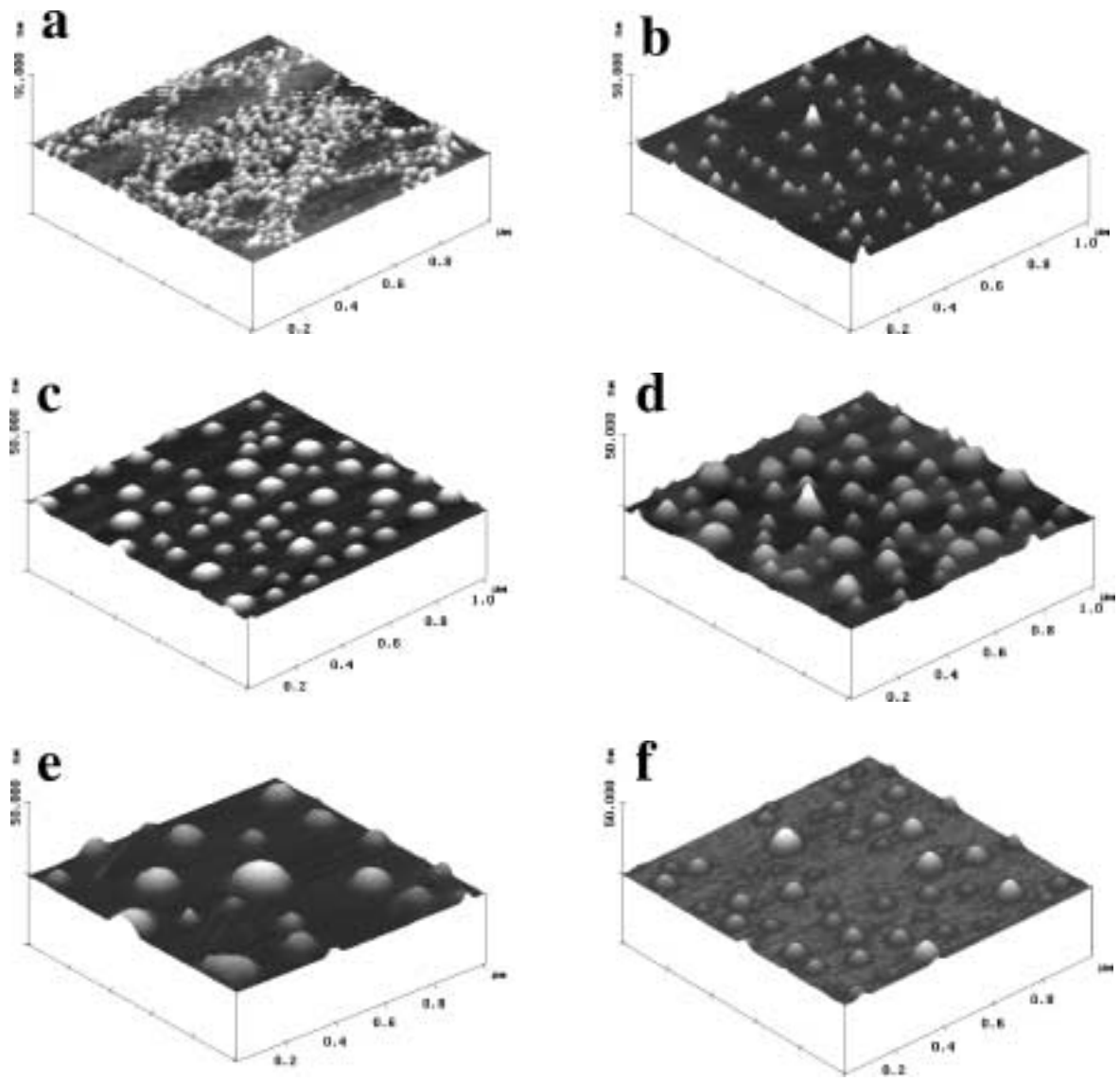

Figure 1. 3D TMAFM images of six kinds of Pt/Co nanoparticles electrodeposited at 1 μA for 3 s from mixed aqueous solutions of (a) 2.5 mM H_2PtCl_6/5 mM $CoCl_2$; (b) 2.5 mM H_2PtCl_6/50 mM $CoCl_2$; (c) 2.5 mM H_2PtCl_6/100 mM $CoCl_2$; (d) 2.5 mM H_2PtCl_6/150 mM $CoCl_2$; (e) 2.5 mM H_2PtCl_6/50 mM $CoCl_2$ but at 100 μA for 3 s after air annealing, (f) 2.5 mM H_2PtCl_6/80 mM Et_4NCl acetonitrile solution.

scan depends on the limit of the high potential and whether intermediates formed were oxidized. Similar experience is observed here and in particular, when the highest applied potential is less than 800 mV Ag/AgCl, only one forward peak is observed and has roughly the same height and location as the peak during reverse scan. This is also reported in figure 20(a) of Capon and Parsons [15]. Sodium formate in perchloric acid has a higher pH than formic acid in perchloric acid of the same concentration and their CV are slightly different. Figure 3 shows the CV of a control scan of the microelectrode in perchloric acid without sodium formate. No oxidation peaks were observed and the hydrogen evolution region is about 200 mV higher than for the acidified formate solution in figure 2, due to difference in pH.

Similar shapes of cyclic voltammograms were observed for formic acid oxidation on Pt and Pt/Co nanoparticles on HOPG. Figure 4 shows the CVs of Pt/Co nanoparticles with different composition. As opposed to figure 2, a lower value of 700, 750, or 800 mV Ag/AgCl was used as the high potential limit. Only one oxidation peak is observed in the forward scan and the oxidation in the reverse scan follow closely the track of the forward scan. This CV is similar to figure 20(a) of [15] and is quite reproducible. Two cycles of CV were performed in each of the nanoparticle kinetic experiment and only the second cycle is recorded and shown. In figure 4, the oxidation peak potentials of the various Pt/Co nanoparticles vary slightly and are within 50 mV. The peak currents, however, vary greatly with the Pt/Co composition of the nanoparticles. The oxidation peak current densities of the various samples in table 1 were determined and tabulated in the last row. Figure 4 shows that the maximum peak current density is for Pt/Co particles with a composition of

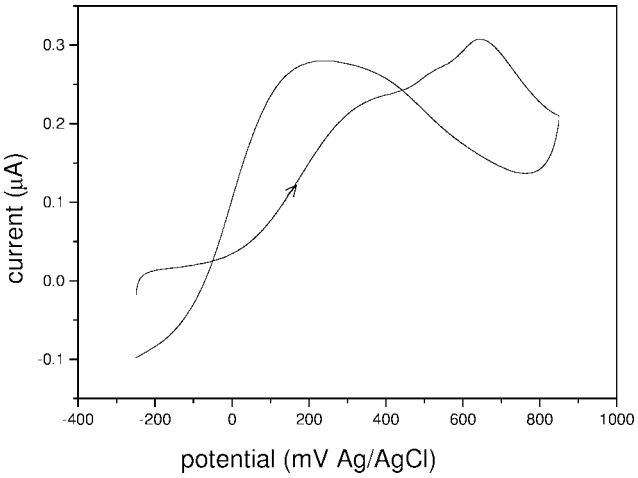

Figure 2. Cyclic voltammogram of a 100 μm diameter Pt microelectrode in 0.2 M HCOONa/0.28 M $HClO_4$ solution with a scan rate of 100 mV/s. The full range of potential scan is shown with the lower and upper limits.

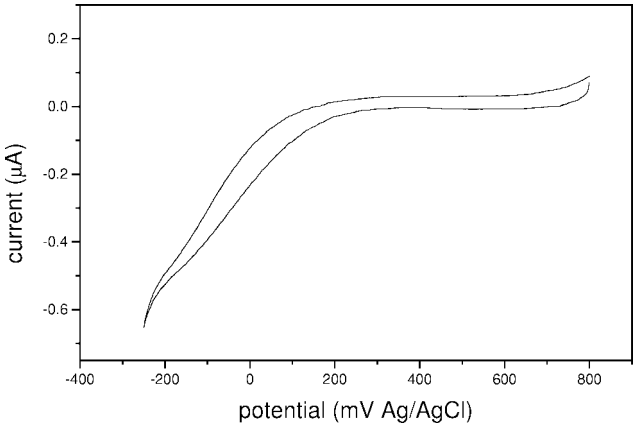

Figure 3. Cyclic voltammogram of a control experiment for the same set up as in figure 2 but without the sodium formate. The hydrogen region is shifted positive because of a lower pH in the 0.28 M perchloric acid.

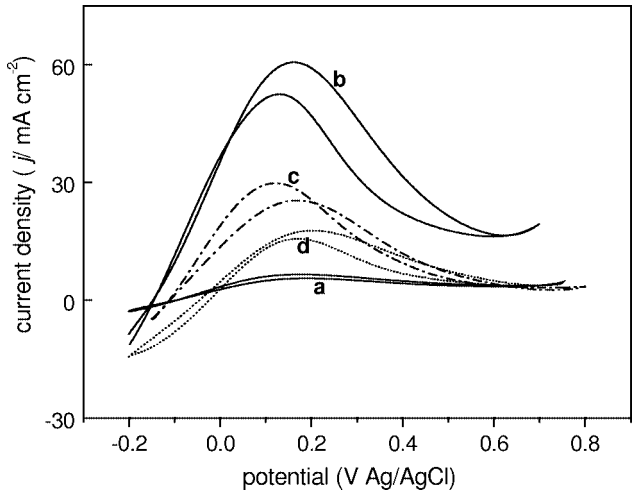

Figure 4. Cyclic voltammogram for formic acid oxidation (0.2 M HCOONa/0.28 M $HClO_4$) on Pt/Co nanoparticles at a scan rate of 20 mV/s. (Curves are (a) 33.2, (b) 77.6, (c) 81.6, and (d) 88.1 at% Co, respectively). The full range of potential scan and the second cycle of the CV for each curve is shown.

Pt : Co atom ratio of 1 : 1.1–1 : 3.5. The maximum peak current density is about one order of magnitude higher than that of pure Pt particles.

One possible explanation for the enhanced activity of the bimetallic particles is the bi-function effect of platinum and cobalt [7]. One possible role of cobalt in promoting the catalysis of platinum, is the removal of CO_{ad} on adjacent platinum atoms. Cobalt atoms are carrying oxygen-containing species and are able to oxidize the poison intermediates, CO_{ad} and reactive intermediate, $COOH_{ad}$, at a potential lower than that for pure platinum. The actual morphology and mixing of platinum and cobalt at the atomic level is therefore critical in maximizing the catalysis rate for steps (2)–(5). Characterization of the Co composition at the nanoparticle level provides a reasonable way to find the optimal Pt : Co ratio for balancing the formation of COOH by platinum and removal of intermediates by cobalt. From our results, the optimum Co composition in the bimetallic particles is between 53 and 78%. This corresponds to roughly one Pt atom to 1–3.5 Co atoms.

In table 1, the Pt/Co nanoparticles with different compositions also have different sizes after the standard electrochemical deposition procedure. Under the same deposition conditions, there is a small correlation of larger particles with higher Co concentration. The variation of oxidation activity with Co composition could be due to this size effect. In order to investigate this possibility, larger particles of 1 : 3.46 Pt : Co composition were prepared by longer deposition times using the same deposition bath. Pt/Co nanoparticles with a mean diameter of about 89.7 nm were prepared from 2.5 mM H_2PtCl_6/50 mM $CoCl_2$ at 100 μA for 3 s and with air annealing. About the same peak current density 55 mA/cm^2 was observed and is very near to that of the smaller Pt/Co nanoparticles. Apparently, no quantum size effects were observed, as our particles prepared are not small enough for quantum size effects to become apparent. Characterization of very small Pt/Co and Pt nanoparticles on HOPG is difficult with the TMAFM. Although better resolution can be obtained with contact mode AFM, interaction of the AFM tip with the loosely adsorbed nanoparticles precludes contact mode operation.

Our present results do not show unusual kinetic behaviour for the Pt/Co nanoparticles over the size range we examined. One advantage of using nanoparticles for kinetics study of bimetallic catalysis is that the composition characterization can be done at the nanoparticle level. The other advantage is that mass-transfer and diffusion effects (that usually mask true intrinsic kinetics of catalysis) are absent. It is known that mass-transfer resistance reduces as one goes from wire electrodes to microcylinder or microdisk electrodes. To investigate and compare the mass-transfer effects, cyclic voltammograms of formic acid oxidation were performed on various wire electrodes and microelectrodes. For a wire electrode in dimensions of mm, the current response is based on planar diffusion (Cottrell equation) [16] and is independent of the dimension of the wire. For microelec-

trodes, spherical diffusion is significant and the current density increases linearly with $1/r_0$ [16] as given by

$$j_{\text{spherical}} = j_{\text{planar}} + \frac{nFD_0C^0}{r_0}, \qquad (6)$$

where j_{planar} is the planar peak current density, r_0 is the radius of the electrode, n is the number of electrons transferred in the electrode reaction, and C^0 is the bulk concentration of electroactive species. The units for D_0, C^0 and r_0 are cm^2/s, mol/cm^3, and cm, respectively.

Figure 6 plots the peak current density, j_p (mA/cm^2) variation with the characteristic dimension of the electrode in $1/r_0$ (1/cm) for formic acid on Pt wire, Pt microelectrodes, and Pt nanoparticles. In the various electrode geometries, r_0 represents the radius of a wire, the radius of the disk in a microelectrode, and the radius of the nanoparticles.

In the upper panel of figure 6, pure Pt nanoparticles of various sizes show the same peak oxidation current, indicating the absence of mass-transfer effects according to equation (6). In the middle panel, a linear relationship of j_p versus $1/r_0$ is shown in qualitative agreement with equation (6) for the microelectrodes. The sizes of the Pt microelectrodes are ∅ 10, 50, and 100 μm. In the bottom panel, no $1/r_0$ dependence was found. The Pt wires have sizes ∅ 0.222, 0.424, 1.175, and 1.66 mm. This indicates that planar diffusion is predominant. Using values of $n = 2$, $D_0 = 10^{-5}$ cm^2/s, $F = 10^5$ Coul/mol, $C^0 = 0.2$ mol/1000 cm^3, $r_0 = 25\times10^{-4}$ cm, the spherical diffusion limiting current is 160 mA/cm^2 from equation (6) for the case of a 50 μm diameter microelectrode. Similar values can be calculated from the Nicholson and Shain equation for the peak current density in a CV on a planar electrode. This is about twenty times higher than the peak current density in figure 6. It is possible that n is 1 in the rate-determining step, e.g., equation (2) and the diffusion coefficient of formic acid or formate could be one order of magnitude smaller. The other possible explanation of the quantitative discrepancy could be due to the concentration of the active diffusing species. If the dissociated anion $HCOO^-$ is the electroactive species, its concentration will be significantly lower than 0.2 molar since the dissociation constant of formic acid is 1.77×10^{-4}. While further quantitative analyses are necessary to clarify this point, we simply reported that mass-transfer effects are observed in the microelectrodes but not for the nanoparticles.

Figure 7 gives us an overall view of all the peak current, j_p (mA/cm^2) versus $1/r_0$ (1/cm) for formic acid oxidation on these three kinds of electrodes with different scan rates in stirred solutions. It is further verified that the mass-transfer controlled linear dependence of current in microelectrodes can be removed by stirring, whereas stirring has no effect on the current in nanoparticles. The linear dependence of current with scan rate also shows that the kinetics observed is the intrinsic electrocatalytic activity of platinum. The current density representing the intrinsic kinetics is 6.1 mA/cm^2 at a scan rate of 20 mV/s. For 5 mV/s, the current densities are around 5.2 mA/cm^2. For 100 mV/s, the current densities are around 7.8 mA/cm^2.

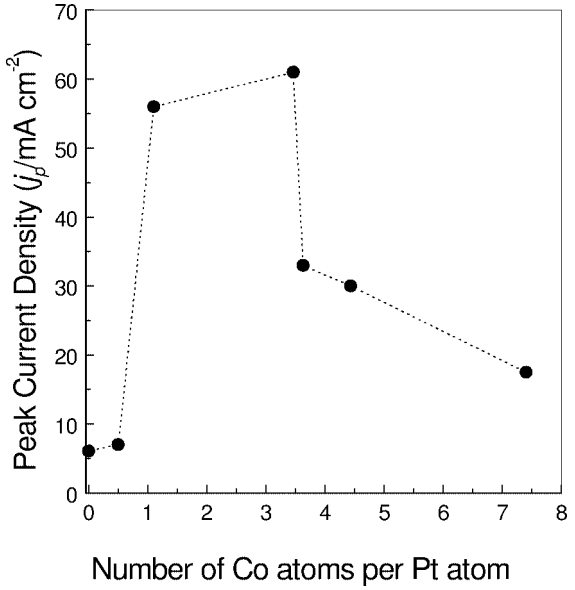

Figure 5. The peak current density of formic acid oxidation (0.2 M HCOONa/0.28 M $HClO_4$, scan rate 20 mV/s) as a function of Co at% in a Pt/Co mixture.

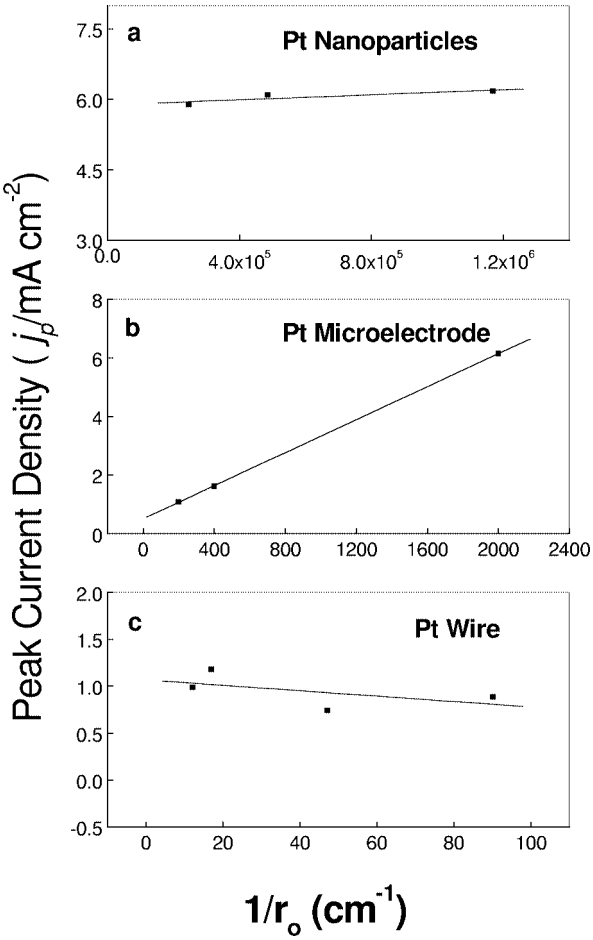

Figure 6. The changes of peak current density, j_p (mA/cm^2) with $1/r_0$ (1/cm) for formic acid oxidation (0.2 M HCOONa/0.28 M $HClO_4$, scan rate 20 mV/s) on (a) Pt nanoparticles in figure 1(f), (b) Pt microelectrodes (∅ 10, 50, and 100 μm) and (c) Pt wires (∅ 0.222, 0.424, 1.175, and 1.66 mm).

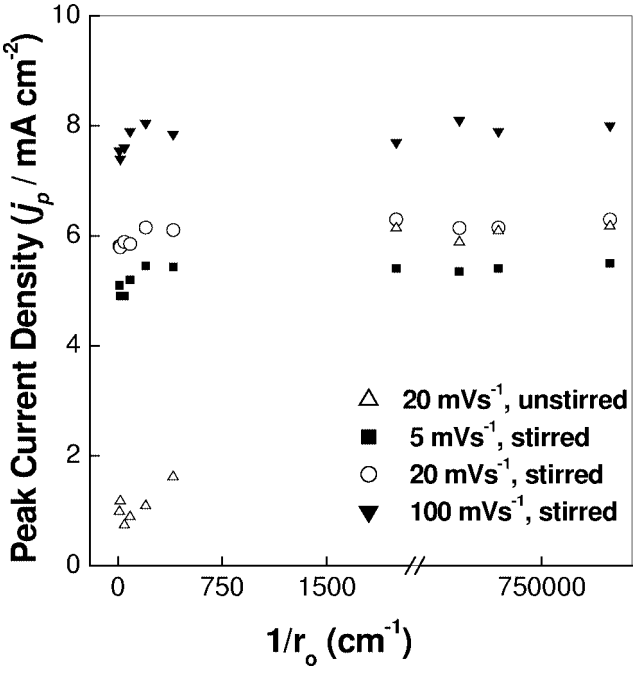

Figure 7. The changes of peak current density, j_p (mA/cm^2) with $1/r_0$ (1/cm) for formic acid oxidation (0.2 M HCOONa/0.28 M $HClO_4$) on three kinds of electrodes with different scan rate in stirred solution.

4. Conclusions

The current response behavior for formic acid oxidation on Pt and Pt/Co nanoparticles is kinetics controlled and free from mass transfer effects. Co modification of Pt nanoparticles can enhance the kinetics of formic acid oxidation. Different Co loading of Pt/Co nanoparticles can strongly influence the catalytic activity, which is related to the balance between the electro-oxidation rate and adsorption rate of formic acid. The optimum composition is between 1 : 1.1 and 1 : 3.5 Pt : Co atom ratio in the bimetallic nanoparticles and it gives a maximum catalytic activity (55–61 mA/cm^2) for formic acid oxidation.

Acknowledgement

Financial support by the Research Grants Council (HKU 7089/98P) of Hong Kong is acknowledged. KYC also acknowledges University of Hong Kong's Outstanding Researcher Award (1998).

References

[1] M. Peuckert, T. Yoneda, R.A. Dalla Betta and M. Boudart, J. Electrochem. Soc. 133 (1986) 944.
[2] K. Kinoshita, J. Electrochem. Soc. 137 (1990) 845.
[3] I. Lee, K.Y. Chan and D.L. Phillips, Appl. Surf. Sci. 136 (1998) 321.
[4] I. Lee, K.Y. Chan and D.L. Phillips, Ultramicroscopy 75 (1998) 69.
[5] J.V. Zoval, J. Lee, S. Gorer and R.M. Penner, J. Phys. Chem. B 102 (1998) 1166.
[6] A. Kelaidopoulou, E. Abelidou and G. Kokkinidis, J. Appl. Electrochem. 29 (1999) 1255
[7] H.A. Gasteiger, Electrochem. Soc. Interface, Fall (1994) 49.
[8] H.A. Gasteiger, N.M. Markovic, P.N. Ross, Jr. and E.J. Cairn, Electrochim. Acta 39 (1994) 1825.
[9] W. Chrzanowski and A. Wieckowski, Langmuir 14 (1998) 1967.
[10] H.A. Gasteiger, N.M. Markovic and P.N. Ross, Jr. J. Phys. Chem. 99 (1995) 8945.
[11] A. Kelaidopoulou, E. Abelidou, A. Papoutsis, E.K. Polychroniadis and G. Kokkinidis, J. Appl. Electrochem. 28 (1998) 1101.
[12] X.H. Xia and T. Iwasita, J. Electrochem. Soc. 140 (1993) 2559.
[13] A. Capon and R. Parsons, J. Electroanal. Chem. 44 (1973) 1.
[14] H. Kita, T. Katagiri and K. Kunimatsu, J. Electroanal. Chem. 220 (1987) 125.
[15] A. Capon and R. Parsons, J. Electroanal. Chem. 45 (1973) 205.
[16] A.J. Bard and L.R. Faulkner, *Electrochemical Methods Fundamentals and Applications* (1980).